Journal of Colloid and Interface Science 542 (2019) 387–391

Contents lists available at ScienceDirect

Journal of Colloid and Interface Science

journal homepage: www.elsevier.com/locate/jcis

Short Communication

Electrochemically modified graphite for fast preparation of large-sized graphene oxide

Peng He [a,b,1], Jiushun Zhou [a,b,1], Huixia Tang [a,b], Siwei Yang [a,b], Zhi Liu [a,b,c,*], Xiaoming Xie [a,b,c], Guqiao Ding [a,b,*]

[a] State Key Laboratory of Functional Materials for Informatics, CAS Center for Excellence in Superconducting Electronics (CENSE), Shanghai Institute of Microsystem and Information Technology, Chinese Academy of Sciences, Shanghai 200050, PR China
[b] College of Materials Science and Opto-Electronic Technology, University of Chinese Academy of Sciences, Beijing 100049, PR China
[c] School of Physical Science and Technology, ShanghaiTech University, Shanghai 200031, PR China

GRAPHICAL ABSTRACT

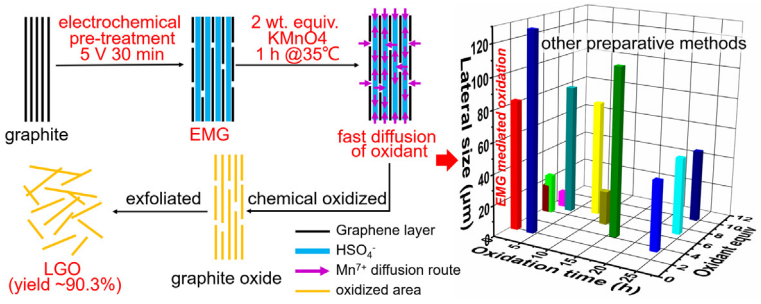

ARTICLE INFO

Article history:
Received 24 December 2018
Revised 7 February 2019
Accepted 7 February 2019
Available online 8 February 2019

Keywords:
Graphene oxide
Electrochemical pre-treatment
Large size
Fast chemical oxidation

ABSTRACT

Large-sized graphene oxide (LGO) is desirable for many graphene-based applications. Herein, for the first time, we synthesized LGO (83 μm average size) using electrochemically modified graphite as the precursor. With this strategy, we could reduce both the oxidation time (1 h) and oxidant dosage (2 equiv.) while achieving a fast and high-yield (~90.3 wt%) LGO preparation. LGO papers show much better mechanical properties and nearly four times higher conductivity (after reduction) than their counterparts assembled using small-sized GO. The results demonstrated that electrochemical pre-treatment is an efficient approach to accelerate the oxidation of graphite at low oxidant dosages and to control the size of the resulting GO.

1. Introduction

Graphene oxide (GO), which is a derivative of graphene and possesses various oxygen-containing functional groups, exhibits unique properties such as excellent processability and good flexibility for functionalization [1]. GO sheets with large lateral size show strong interactions, less edge contact, and high orientation, which improve the conductivity [2], mechanical strength [3], and liquid crystal properties [4] of the corresponding macroscopic materials. However, the fast preparation of large-sized GO (LGO) with high-yield is challenging. The conventional methods used for preparing LGO sheets larger than 50 μm in size suffer from long time oxidation times (up to 6 h [5]), high oxidant usages (up to 6 equiv. [6]), and/or and low yield (as low as 4.3 wt% [7]). According

* Corresponding authors at: State Key Laboratory of Functional Materials for Informatics, CAS Center for Excellence in Superconducting Electronics (CENSE), Shanghai Institute of Microsystem and Information Technology, Chinese Academy of Sciences, Shanghai 200050, PR China.
E-mail addresses: zliu2@mail.sim.ac.cn (Z. Liu), gqding@mail.sim.ac.cn (G. Ding).
[1] These authors contribute equally to this work.

https://doi.org/10.1016/j.jcis.2019.02.029
0021-9797/

to Dong et al. [8], the diffusion rate of oxidants between the graphite interlayers, rather than the oxidant dosage, affects the oxidation of graphite. More importantly, a high oxidant dosage causes severe oxidative fragmentation of the sheets, reduces the LGO yield, causes environmental pollution, and renders the preparation process dangerous. Lu et al. recently achieved high-yield (100 wt%) preparation of LGO (108 μm in average) by expanding the interlayer spacing of graphite for fast oxidant diffusion. The reaction required an oxidation time of only 4 h and only 2 equiv. $KMnO_4$ was used as the oxidant [9]. This work represents a significant progress in the fast oxidation of graphite for preparing LGO. However, this method requires the chemical expansion of graphite, which is a tedious (requires more than 20 h) and dangerous process [9,10]. Various electrochemical methods have been proposed for fast and scalable GO fabrication without using any additional oxidant. However, the size of GO obtained using these approaches is limited to several micrometers [11]. Hence, the fast and high-yield preparation of LGO at low oxidant dosages remains challenging.

Herein, we propose a method to prepare LGO using electrochemically modified graphite (EMG). The physicochemical characterization results confirmed the successful preparation of LGO. The oxidation mechanism was investigated to elucidate the role of electrochemical treatment in the fast oxidant diffusion and oxidation of graphite. To the best of our knowledge, such an electrothermal approach has never been used to speed up the chemical oxidation process for efficient LGO fabrication.

2. Results and discussion

The schematic of the LGO preparation process used in this study is shown in Fig. 1, and a detailed description of the process is given in Experimental Section of the Supporting Information. The LGO preparation involved three steps: the formation of EMG by electrochemical treatment, chemical oxidation of graphite, and extraction of graphene oxide by purification and exfoliation. The last step involves mesh-filtration, sediment cleaning, and shanking [9], which are more time-consuming than many conventional techniques such as filtration, centrifugation, and dialysis. More importantly, since both the electrochemical treatment and chemical oxidation of graphite were carried out in the same liquid medium (concentrated sulfuric acid), the EMG prepared in the first step (blue powder floating on the surface of the electrolyte) could be directly utilized in the second step. The first two steps required only 1.5–2 h and 2 equiv. $KMnO_4$ to complete the oxidation of graphite. Hence, this method is better than the previously reported methods in terms of efficiency provided it produces GO sheets with large size and reasonably high yield.

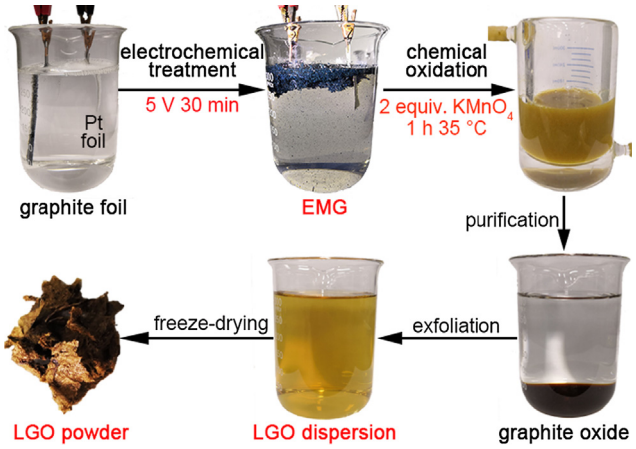

Fig. 1. EMG-mediated LGO preparation.

Scanning electron microscopy (SEM) and atomic force microscopy (AFM) were employed to analyze the lateral size and thickness of the resulting sheets. From the SEM images (Figs. 2a and S1a–c) of the sheets it can be observed that most of them were larger than 50 μm in size. Sheets larger than 250 μm in size (Fig. S1c) could also be observed. The statistical analysis of 200 isolated GO sheets revealed that their average lateral size was 83 μm and 85% of them were larger than 50 μm (Fig. 2b). The AMF images and distribution histograms (Fig. 2c and S1d–g) show that the isolated sheets had a thickness in the range of 1–5 nm corresponding to single layer and few-layered sheets [6]. The statistical analysis of 100 sheets (Fig. 2d) revealed that 80% of them were monolayer and bilayer, indicating in combination with the SEM results that the as-prepared LGO powder consisted of large and thin sheets. The Raman spectrum of the sheets showed a strong D peak at 1351 cm^{-1} (Fig. 1e). The mapping of the I_D/I_G of the sheets shown in Fig. 1e and its value of 1.15–1.23 suggest that structural defects were homogeneously distributed in the sheets. This is consistent with the transmission electron microscopy and selected area electron diffraction results (Fig. S2), which indicated that the sheets were amorphous in nature. The X-ray photoelectron spectroscopy (XPS, Fig. 2f) results showed that the sheets had a C/O atomic ratio of ~1.94 and consisted of oxygen-containing groups including epoxy/hydroxyl (C—O, 286.8 eV), carbonyl (C═O, 288 eV), and carboxyl (O-C═O, 289.1 eV) [12], which were responsible for the structural defects detected by Raman spectroscopy. These results are consistent with the Fourier transform infrared spectroscopy (FT-IR) and thermogravimetric analysis (TGA) results. The FT-IR spectrum of the sheets showed peaks corresponding to carbon-oxygen groups (C—O at 1046, 1088, and 1402 cm^{-1}, C═O at 1724 cm^{-1}) (Fig. S3a). The TGA results revealed that the sheets showed a weight loss of 31.42% at 150–300 °C (Fig. S3b), corresponding to the pyrolysis of the abovementioned oxygen-containing groups [13]. The morphological, structural, and chemical compositional analyses confirmed the successful preparation of LGO in both the dispersion and powder forms. The yield of the obtained LGO powder was calculated (average of 10 batches) to be 90.3 wt%. The prepared samples showed properties characteristic of LGO, also confirming the successful preparation of LGO sheets. The aqueous dispersion of the obtained LGO sheets (0.5 mg/mL) exhibited spreading Schlieren textures (Fig. 2g) under a polarized optical microscope (POM) (as observed in previous studies), indicating the formation of a stable nematic liquid crystal because of the large size induced self-alignment of the sheets [4]. This liquid crystal phenomenon became predominant with an increase in the LGO concentration (in the dispersion) to 2 and 5 mg/mL (Fig. S4). The aqueous dispersion could also be processed into free-standing and foldable papers (Fig. 2h) with a smooth surface (Fig. 2i) and compact layered microstructure (Fig. 2j). From the strain-stress curves shown in Fig. 2k, it can be observed that the LGO papers showed higher Young's modulus (12.2 GPa) and tensile strength (156.3 MPa) than the papers prepared from traditionally prepared small-sized graphene oxide (SGO) with an average lateral size of 2.9 μm (Fig. S5). This is because the LGO papers consisted of fewer weak interlayer junctions than SGO papers. Reduced interlayer junctions also decrease the interlayer contact resistance between neighboring sheets. Hence, the hydroiodic acid reduced (HI-reduced) LGO papers showed a nearly four times higher conductivity (38760 S/m) than HI-reduced SGO papers (10989 S/m). The much better mechanical strength and electrical properties of these LGO papers demonstrate their potential for practical applications.

We compared the efficiency of various LGO preparation methods with the method used in this study (Fig. S6a). The EMD-mediated oxidation route we proposed in this study was found to be worse only than those used in Refs. [9,14] in terms of the lat-

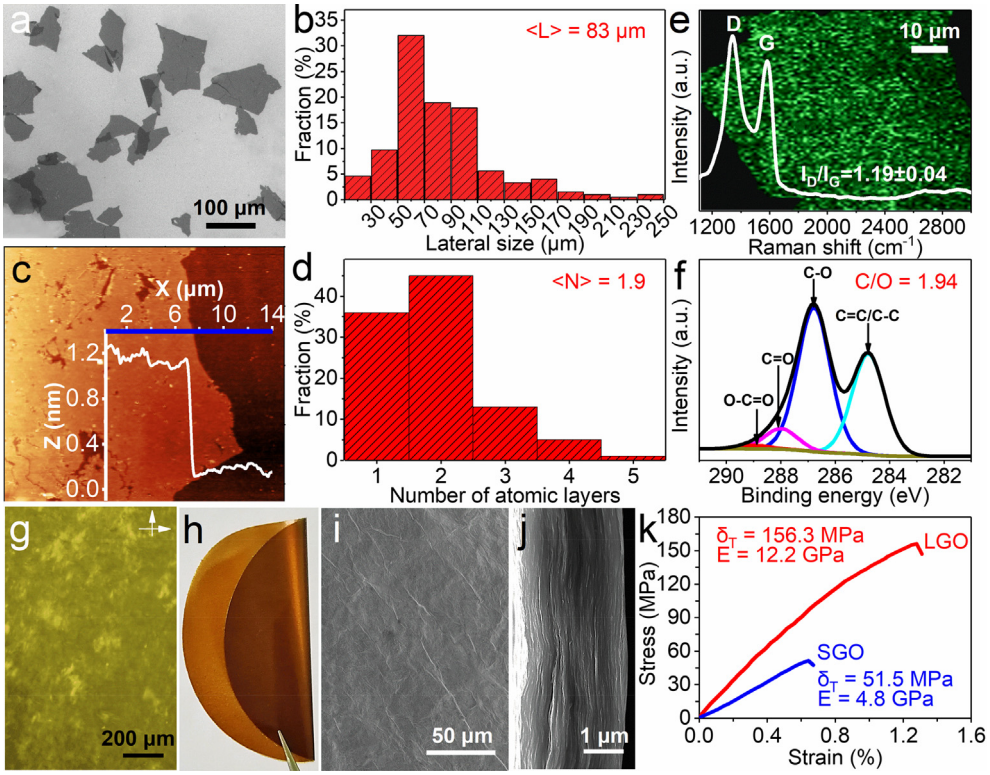

Fig. 2. Characterization of LGO. Typical SEM image (a), lateral size distribution histogram (b), AFM image with the height profile (c), thickness distribution histogram (d), Raman spectrum (e), C 1s XPS spectrum (f); (g) POM of LGO dispersion (0.5 mg/mL); Photograph (h), surface (i) and cross-sectional (j) SEM images of LGO paper; (k) Strain-stress curves of LGO paper (red) and SGO paper (blue). (For interpretation of the references to colour in this figure legend, the reader is referred to the web version of this article.)

eral size and yield. Our method required very low oxidant dosage and short oxidation time, and hence is an efficient and green strategy for the preparation of LGO larger than 50 μm in size (Fig. S6b). Considering the similar purification and exfoliation procedures, the advantage of our method would be more obvious when we calculate both the oxidation duration and the time taken before oxidation (Table S1). The electrochemical treatment in our method required only 30 min, while the pre-treatment step in Ref. [9] required 20 h though the oxidant consumption for the chemical oxidation in this method was as low as 2 equiv. (Table S1). The reasonably high LGO yield obtained in this study indicates the feasibility of our electrochemical treatment (in combination with chemical oxidation) method for fast oxidation of graphite with low oxidant usage. To probe the underlying mechanism, we compared the oxidation of EMG and graphite under the same oxidation conditions (2 equiv. oxidant and 35 °C). The XRD spectra of the samples oxidized for different durations (0, 5, 15, 30, 60 min) (Fig. 3a and b) show that the interlayer distance of EMG increased with the formation of oxygen-containing groups, indicating the evolution of graphite to graphite oxide. After 1 h of oxidation, EMG completely lost its graphitic characteristics (peak at 26.6° (0 0 2)), indicating a uniform and complete oxidation. On the other hand, in the case of graphite, the peak at 26.6° could be observed (though weaker than the characteristic peak of graphite oxide (around 9.6°)) even after 1 h of oxidation. This suggests the oxidation of graphite was slower than that of EMG. A further increase in the oxidation time (of graphite) to 2 h resulted in slight variations in the d-spacing (Fig. S7a), and the resulting product consisted of a few large and thick sheets with incompletely oxidized center areas (Fig. S7b, c). The faster and more uniform oxidation of EMG than that of graphite demonstrates the importance of electrochemical pre-treatment and modifying the structure of graphite (to produce EMG) for accelerating its chemical oxidation process. We investigated the changes in the structure of graphite during the electrochemical pre-treatment. Both the XRD (Fig. 3c) and Raman (Fig. 3d) results revealed that EMG showed stage-I intercalation [11]. This is consistent with the blue color of EMG (Fig. 1). However, when this blue EMG was washed with water, de-intercalation occurred, as indicated by the grey color of the resulting powder (labeled as DI-EMG). Unlike graphite, DI-EMG showed a strong wide XRD peak at $2\theta = 26.6°$ and a strong D peak in the Raman spectrum (an increased I_D/I_G of ~0.89), indicating the presence of structural defects in it. XPS data, C1 spectrum and FT-IR spectra (Figs. S8a–c) show that DI-EMG possessed a larger number of oxygen-containing groups and lower C/O ratio than graphite, indicating the mild oxidation of DI-EMG. Since graphite cannot be oxidized by simple water washing, it can be stated that the structural defects originated from the electrochemical process. Graphite is vulnerable to concentrated sulfuric acid when positive direct electrical current (DC) voltage is applied because the intercalation is often accompanied by the generation of reactive radicals (e.g. hydroxyl radical) and bubbles (Figs. S8d and e) between the graphite interlayers [11]. These radicals and bubbles generate oxygen-containing groups, cracks and/or holes on both the surface and internal layers of graphite. Therefore, we believe that these defects in EMG facilitated the oxidant diffusion, leading to fast oxidation. This was confirmed by the micromorphology (observed using an optical microscope) of the intermediate products obtained after the 30 min chemical oxidation of EMG and graphite. The luminous and dark regions correspond to the adequately oxidized and unoxidized/partially oxidized areas, respectively. As shown in Fig. S9a, the oxidation of graphite sheets occurred preferentially from the edgy area, indicative of an edge-to-center diffusion route of the oxidant. However, in the case of EMG, the oxidation started

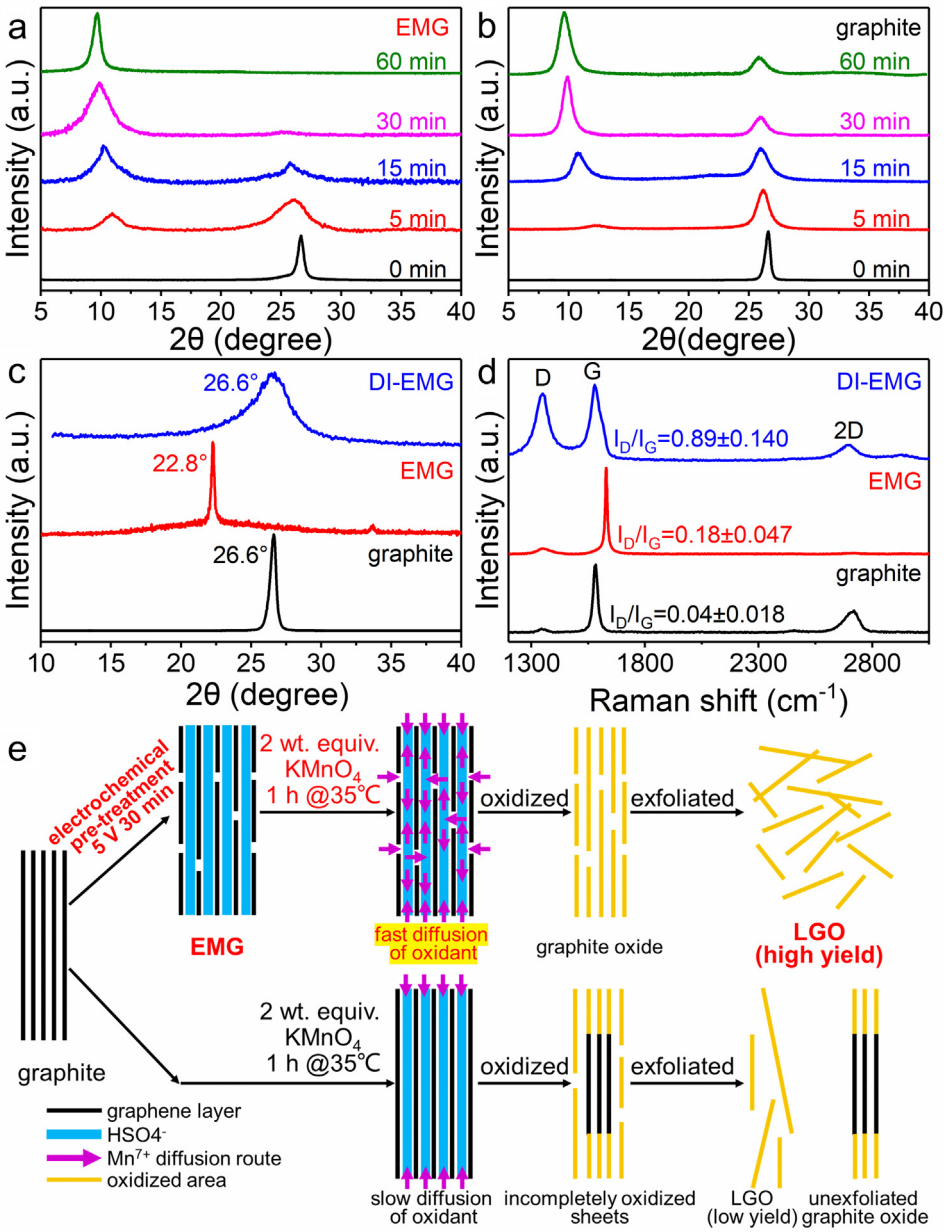

Fig. 3. XRD patterns of the products obtained after 0, 5, 15, 30, and 60 min of EMG (a) and graphite (b) oxidation; XRD patterns (c) and Raman spectra (d) of graphite, EMG, and DI-EMG; (e) Schematic of the EMG-mediated fast oxidation process.

from both the edgy and center regions (Fig. S9b). Cracks and holes were also observed, as indicated by the red arrows in Fig S9b. Hence, it can be stated that with an increase in the number of diffusion channels/routes, the structural defects made the center and internal areas of EMG more accessible to the oxidant, thus enabling a fast chemical oxidation mode (simultaneous edge and center oxidation) different from the case of untreated graphite (edge-to-center oxidation). It should be noted that these electrochemically-derived cracks and holes do not lead to the complete fragmentation of sheets, thus producing small-sized GO. Fig. 3e illustrates the mechanism of the EMG-mediated fast oxidation of graphite. The electrochemically-derived structural defects increased the number of oxidant diffusion channels, changed the oxidation mode, and accelerated the oxidation process. According to this mechanism, modulating the defect content is also important because a large number of densely distributed defects can reduce the sheet size significantly. Therefore, by properly controlling the defects generated during the electrochemical process (will be carried out in our future work), larger size GO with higher yield can be obtained by fast oxidation of EMG at low oxidant dosages.

3. Conclusion

To overcome the limitations of large oxidation time and oxidant dosages of the previously reported LGO preparation methods [5–7,9–11], we proposed an EGM-mediated approach for fast LGO preparation. By introducing an electrochemical treatment, the graphite structure could be modified (micron scale-cracks and holes). These modifications were found to effective in increasing the accessibility of the internal two-dimensional galleries of large graphite flakes and accelerating the oxidant diffusion in them, thus facilitating the fast oxidation at low oxidant dosages. Using this approach, EGM could be adequately oxidized at a very

low oxidant dosage (2 equiv.) within 1 h to form LGO with a mean size of 83 μm and a yield of 90.3 wt%. The LGO papers showed much better mechanical properties (Young's modulus of 12.2 GPa, tensile strength of 156.3 MPa) and a nearly four times higher conductivity (38760 S/m after hydroiodic acid reduction) than SGO papers. This method involving electrochemical modification and chemical oxidation provides an eco-friendly strategy for highly efficient production of LGO.

Funding

This work was supported by the National Natural Science Foundation of China (Grants 51802337, 11774368 and 11804353), China Postdoctoral Science Foundation (Grant BX201700271) and STCSM (18511110600).

Appendix A. Supplementary material

Supplementary data to this article can be found online at https://doi.org/10.1016/j.jcis.2019.02.029.

References

[1] Y.W. Zhu, S. Murali, W.W. Cai, X.S. Li, J.W. Suk, J.R. Potts, et al., Graphene and graphene oxide: synthesis, properties, and applications, Adv. Mater. 22 (35) (2010) 3906–3924, https://doi.org/10.1002/adma.201001068.
[2] Q.B. Zheng, W.H. Ip, X.Y. Lin, N. Yousefi, K.K. Yeung, Z.G. Li, et al., Transparent conductive films consisting of ultra large graphene sheets produced by langmuir-blodgett assembly, ACS Nano 5 (7) (2011) 6039–6051, https://doi.org/10.1021/nn2018683.
[3] C.S. Xiang, C.C. Young, X. Wang, Z. Yan, C.C. Hwang, G. Cerioti, et al., Large flake graphene oxide fibers with unconventional 100% knot efficiency and highly aligned small flake graphene oxide fibers, Adv. Mater. 25 (33) (2013) 4592–4597, https://doi.org/10.1002/adma.201301065.
[4] Z. Xu, C. Gao, Aqueous liquid crystals of graphene oxide, ACS Nano 5 (4) (2011) 2908–2915, https://doi.org/10.1021/nn200069w.
[5] X.F. Zhou, Z.P. Liu, A scalable, solution-phase processing route to graphene oxide and graphene ultralarge sheets, Chem. Commun. 46 (15) (2010) 2611–2613, https://doi.org/10.1039/b914412a.
[6] J.P. Zhao, S.F. Pei, W.C. Ren, L.B. Gao, H.M. Cheng, Efficient preparation of large-area graphene oxide sheets for transparent conductive films, ACS Nano 4 (9) (2010) 5245–5252, https://doi.org/10.1021/nn1015506.
[7] C.Y. Su, Y.P. Xu, W.J. Zhang, J.W. Zhao, X.H. Tang, C.H. Tsai, et al., Electrical and spectroscopic characterizations of ultra-large reduced graphene oxide monolayers, Chem. Mater. 21 (23) (2009) 5674–5680, https://doi.org/10.1021/cm902182y.
[8] L. Dong, J. Yang, M. Chhowalla, K.P. Loh, Synthesis and reduction of large sized graphene oxide sheets, Chem. Soc. Rev. 46 (23) (2017) 7306–7316, https://doi.org/10.1039/c7cs00485k.
[9] L. Dong, Z.X. Chen, S. Lin, K. Wang, C. Ma, H.B. Lu, Reactivity-controlled preparation of ultralarge graphene oxide by chemical expansion of graphite, Chem. Mater. 29 (2) (2017) 564–572, https://doi.org/10.1021/acs.chemmater.6b03748.
[10] J.H. Ma, P. Wang, L. Dong, Y.B. Ruan, H.B. Lu, Highly conductive, mechanically strong graphene monolith assembled by three-dimensional printing of large graphene oxide, J. Colloid Interface Sci. 534 (2019) 12–19, https://doi.org/10.1016/j.jcis.2018.08.096.
[11] S.F. Pei, Q.W. Wei, K. Huang, H.M. Cheng, W.C. Ren, Green synthesis of graphene oxide by seconds timescale water electrolytic oxidation, Nature Commun. (2018) 9, https://doi.org/10.1038/s41467-017-02479-z.
[12] P. He, J. Sun, S.Y. Tian, S.W. Yang, S.J. Ding, G.Q. Ding, et al., Processable aqueous dispersions of graphene stabilized by graphene quantum dots, Chem. Mater. 27 (1) (2015) 218–226, https://doi.org/10.1021/cm503782p.
[13] J.F. Shen, Y.H. Hu, C. Li, C. Qin, M.X. Ye, Synthesis of amphiphilic graphene nanoplatelets, Small 5 (1) (2009) 82–85, https://doi.org/10.1002/smll.200800988.
[14] J.J. Zhang, Q.Q. Liu, Y.B. Ruan, S. Ling, K. Wang, H.B. Lu, Monolithic crystalline swelling of graphite oxide: a bridge to ultralarge graphene oxide with high scalability, Chem. Mater. 30 (6) (2018) 1888–1897, https://doi.org/10.1021/acs.chemmater.7b04458.